

Hydrophobic molecular similarity from MST fractional contributions to the octanol/water partition coefficient

Jordi Muñoz-Muriedas^{a,†} Samantha Perspicace^{b,e,†} Nuria Bech^a, Salvatore Guccione^b, Modesto Orozco^{c,d,*} & F. Javier Luque^{a,*}

^aDepartament de Fisicoquímica, Facultat de Farmàcia, Universitat de Barcelona, Av. Diagonal 643, 08028, Barcelona, Spain; ^bDipartimento di Scienze Farmaceutiche, Faculty of Pharmacy, University of Catania, viale Andrea Doria 6, Ed. 2, Città Universitaria, I-95125, Catania, Italy; ^cDepartament de Bioquímica i Biologia Molecular, Facultat de Química, Universitat de Barcelona, c/., Martí i Franqués 1, 08028, Barcelona, Spain; ^dUnitat de Modelització Molecular i Bioinformàtica, Institut de Recerca Biomèdica., Parc Científic de Barcelona, c/ Josep Samitier 1, 08028, Barcelona, Spain; ^eOn leave from Dipartimento di Scienze Farmaceutiche, Faculty of Pharmacy, University of Catania, Catania, Italy

Received 5 April 2005; accepted 22 May 2005
© Springer 2005

Key words: molecular similarity, octanol/water partition coefficient, continuum solvation methods, MST model, hydrophobicity, molecular alignment

Summary

The use of a recently proposed hydrophobic similarity index for the alignment of molecules and the prediction of their differences in biological activity is described. The hydrophobic similarity index exploits atomic contributions to the octanol/water transfer free energy, which are evaluated by means of the fractional partitioning scheme developed within the framework of the Miertus-Scrocco-Tomasi continuum model. Those contributions are used to define *global* and *local* measures of hydrophobic similarity. The suitability of this computational strategy is examined for two series of compounds (ACAT inhibitors and 5-HT₃ receptor agonists), which are aligned to maximize the global hydrophobic similarity using a Monte Carlo-simulated protocol. Indeed, the concept of *local* hydrophobic similarity is used to explore structure–activity relationships in a series of COX-2 inhibitors. Inspection of the 3D distribution of hydrophobic/hydrophilic contributions in the aligned molecules is valuable to identify regions of very similar hydrophobicity, which can define pharmacophoric recognition patterns. Moreover, low similar regions permit to identify structural elements that modulate the differences in activity between molecules. Finally, the quantitative relationships found between the pharmacological activity and the hydrophobic similarity index points out that not only the global hydrophobicity, but its 3D distribution, is important to gain insight into the activity of molecules.

Introduction

The prediction of binding modes and affinities of small ligands to biologically relevant target

receptors are important aspects for discovering and optimizing new lead compounds [1]. Unfortunately, in the initial stages of ligand design projects, knowledge of the structure of the target macromolecule is not always available, which implies that information on binding should be indirectly derived from the relationship between the structure

*To whom correspondence should be sent. E-mail: fjlucque@ub.edu, modesto@mmb.pcb.ub.es

[†]J.M.M. and S.P. have contributed equally to this study.

and the activity of a few ligands. In this field methods aimed at examining the similarity between compounds become an useful alternative to ligand design [2]. These methods allow the identification of the molecular features that modulate the biological activity, and from their 3D arrangement a pharmacophore model for the family of compounds under study can be proposed. In turn, this information can be used to search databases with the aim to identify new lead compounds.

Similarity methods score target ligands on the basis of their relative superposition with respect to a reference molecule. Molecular alignment is accomplished by using a variety of approaches, which exploit substructure, geometric and shape features of molecules, as well as the electron density [3–6]. Another approach is based on the comparison of the reactive properties of molecules, like electrostatic potentials and fields calculated at suitable regions around the molecules [7–9]. Particularly, the combined comparison of electrostatic and steric fields in the so-named comparative molecular field analysis (COMFA) has been largely used in drug design studies [10].

The inclusion of the differential solvation properties of molecules in similarity measurements is more elusive, though desolvation is recognized to be one of the major forces that modulate the binding of ligands to the target receptors. Both ligand and receptor binding site are expected to exhibit complementarity in their distribution of hydrophobic/hydrophilic areas. Qualitative descriptions of the distribution of hydrophobic/hydrophilic regions in a molecule can be gained from concepts such as polar/apolar surfaces [11], but those concepts, though chemically intuitive, are arbitrary. Other approaches define the hydrophobicity from atom-based parameters, such as atomic charges, interaction energies with suitable probes, or the free energy surface density [12–14]. Finally, the lipophilicity of a molecule can also be characterized from “lipophilic potentials” [15–17], which are determined by combining fragmental hydrophobic contributions with a distance-dependent function.

Very recently we have proposed a new index to measure the hydrophobic similarity between molecules [18]. This index relies on the partitioning of the free energy of transfer between water and octanol into atomic contributions within the framework of the Miertus-Scrocco-Tomasi (MST) solvation model [19]. The objective of

this work is to examine the suitability of the hydrophobic similarity index as a tool for the alignment of molecules and for predicting bioactivity based on their 3D lipophilicity pattern. To this end, two series of compounds (inhibitors of Acyl-CoA Cholesterol O-Acyl Transferase and agonists of the 5-hydroxytryptamine 3 receptor) are considered to calibrate the suitability of the *global* measure of hydrophobic similarity. Moreover, a third series of compounds (inhibitors of Cyclooxygenase-2) is used to explore the ability of the *local* hydrophobic similarity as a tool to gain insight in structure–activity relationship studies.

Methods

In this section a brief description of the main features of the fractional scheme implemented within the framework of the MST continuum model to derive fractional contribution to the octanol/water partition coefficient is given. Then, the concepts of *global* and *local* measures of hydrophobic similarity between molecules is made. Finally, the three series of compounds considered here are described.

Partitioning of the solvation free energy in the MST continuum model

In the MST method [19] the free energy of solvation is expressed as the addition of three contributions: cavitation, van der Waals, and electrostatic. The cavitation free energy, ΔG_{cav} , is determined following Pierotti's scaled particle theory adapted to molecular shaped cavities by using the procedure proposed by Claverie. Thus, the cavitation free energy of atom i , $\Delta G_{C-P,i}$, is determined weighting the contribution of the isolated atom, $\Delta G_{P,i}$, by the solvent-exposed surface of such an atom, S_i , and the total surface of the molecule, S_T , as noted in Equation 1, where N is the number of atoms.

$$\Delta G_{\text{cav}} = \sum_{i=1}^N \Delta G_{C-P,i} = \sum_{i=1}^N \frac{S_i}{S_T} \Delta G_{P,i} \quad (1)$$

The van der Waals term, ΔG_{vdw} , is computed using a linear relationship to the solvent-exposed surface of each atom, as noted in Equation 2,

where $\Delta G_{\text{vdw},i}$ is the van der Waals free energy of atom i , and ξ_i is the atomic surface tension, which is determined by fitting to the experimental free energy of solvation.

$$\Delta G_{\text{vdw}} = \sum_{i=1}^N \Delta G_{\text{vdw},i} = \sum_{i=1}^N \xi_i S_i \quad (2)$$

The electrostatic contribution, ΔG_{ele} , is determined assuming that the solvent is a continuum polarizable medium, which reacts against the solute charge distribution. Following the original formalism of the Pisa's Polarizable Continuum Model [20], the reaction field generated by the solvent is introduced into the Schrödinger equation by means of a perturbation operator, \hat{V}_R , consisting of a set of imaginary charges located on the solute cavity (Equation 3), which are obtained by solving the Laplace equation with suitable boundary conditions (Equation 4).

$$\hat{V}_R = \sum_{j=1}^M \frac{q_j}{|r_j - r|} \quad (3)$$

where M is the total number of surface elements, j , in which the solute cavity is divided and $\{q_j\}$ denotes the set of charges (located at r_j) that represents the solvent response.

$$q_j = -\frac{\epsilon - 1}{\epsilon} S_j \left(\frac{\partial V_T}{\partial n} \right)_j \quad (4)$$

where V_T is the total electrostatic potential, which includes both solute and solvent contributions, n is the unit vector normal to the surface element j , S_j is the area of the surface element j , and ϵ is the solvent dielectric constant.

Following perturbation theory [21], the electrostatic term can be obtained as half the interaction energy between the charge distribution of the solute in the gas phase with the set of apparent charges corresponding to reaction field created by the fully polarized solvent, $\{q_j^{\text{sol}}\}$ (Equation 5), avoiding the need to introduce the solute Hamiltonian in the definition of ΔG_{ele} . Moreover, Equation 5 allows the partition of ΔG_{ele} into atomic contributions by using the *surface-based* partitioning method [22], as noted in Equation 6

$$\Delta G_{\text{ele}} = \langle \Psi^o | \frac{1}{2} V_R^{\text{sol}} | \Psi^o \rangle \quad (5)$$

where Ψ^o is the wave function of the solute in the gas phase.

$$\Delta G_{\text{ele}} = \sum_{i=1}^N \Delta G_{\text{ele},i} = \sum_{i=1}^N \sum_{\substack{j=1 \\ j \in i}}^M \left\langle \Psi^o \left| \frac{1}{2} \frac{q_j^{\text{sol}}}{|r_j - r|} \right| \Psi^o \right\rangle \quad (6)$$

where the fractional electrostatic contribution of a given atom i , $\Delta G_{\text{ele},i}$, is determined from the interaction energy between the whole charge distribution of the molecule with the apparent charges located at the surface elements pertaining to the portion of the cavity generated from that atom.

Based on the preceding equations, the free energy of transfer between two solvents (for instance, water and octanol; $\Delta G_{\text{w} \rightarrow \text{o}}$) can be expressed in terms of atomic contributions, $\Delta G_{\text{w} \rightarrow \text{o},i}$, which are determined by combining the atomic contributions to the free energy of solvation in the two solvents (Equation 7).

$$\Delta G_{\text{w} \rightarrow \text{o}} = \sum_{i=1}^N \Delta G_{\text{w} \rightarrow \text{o},i} = \sum_{i=1}^N \Delta \Delta G_{\text{ele},i} \\ (+ \Delta \Delta G_{\text{C-P},i} + \Delta \Delta G_{\text{vW},i}) \quad (7)$$

Hydrophobic Similarity

The partitioning of $\Delta G_{\text{w} \rightarrow \text{o}}$ into atomic contributions permits to visualize the 3D distribution of polar/apolar regions in a molecule [18, 23]. Additionally, the information entailed by such atomic contributions can be exploited in more quantitative analysis. Thus, a detailed comparison between the fractional distribution of two molecules (X with N_X atoms, and Y with N_Y atoms) can be obtained from similarity functions like that shown in Equation 8 [18].

$$\Lambda_{XY}(R_{XY}) = \sum_{i=1}^{N_X} \sum_{j=1}^{N_Y} \frac{\Delta G_{\text{w} \rightarrow \text{o},i} \Delta G_{\text{w} \rightarrow \text{o},j}}{(r_{ij}^n + \delta)} \quad (8)$$

where n is an adjustable parameter that controls the shape of the similarity function and δ is a constant that avoids the occurrence of singularities.

Since Λ_{XY} depends on the mutual orientation of molecules X and Y, the optimum orientation is obtained by maximizing Λ_{XY} using simulated

annealing procedures coupled to Monte Carlo simulations combined with optimization procedures. The hydrophobic similarity between molecules can then be determined by using, for example, the Carbó-like index [24], as noted in Equation 9, where Λ_{XX} and Λ_{YY} are self-similarities of molecules X and Y.

$$\gamma_{XY} = \frac{\Lambda_{XY}}{\sqrt{\Lambda_{XX}\Lambda_{YY}}} \quad (9)$$

Equation 9 affords a normalized *global* measure of the hydrophobic similarity between molecules. However, medicinal chemistry studies often deal with series of related compounds that share a common chemical scaffold, where different structural units can be easily identified. In this case, analysis of the differences inherent to each separate unit can be more useful to develop structure–activity relationships than to consider the complete set of chemical modifications in the whole molecule. Thus, for a series of molecules whose structure can be described as the junction of a given number of structural units k ($k=1,\dots,K$), a *local* measure of the hydrophobic similarity for each separate unit can be defined (Equation 10).

$$\gamma_{XY}^k = \frac{\Lambda_{XY}^k}{\sqrt{\Lambda_{XX}^k\Lambda_{YY}^k}} \quad (10)$$

where the similarity function Λ_{XY}^k is evaluated by considering only those fractional contributions pertaining to unit k (Equation 11).

$$\gamma_{XY}^k(R_{XY}) = \sum_{i=1}^{N_X} \sum_{j=1}^{N_Y} \frac{\Delta G_{w \rightarrow o,i} \Delta G_{w \rightarrow o,j}}{(r_{ij}^n + \delta)} \quad (11)$$

Finally, *local* measures of hydrophobic similarity can be related to the differences in biological activity in a series of compounds, as indicated in Equation 12, where the coefficients α_k would provide information about the contribution of each separate unit to the modulation of the biological activity of the whole molecule.

$$\text{Activity} = \sum_k \alpha_k \gamma_{XY}^k \quad (12)$$

Biological systems

The suitability of the hydrophobic similarity as a tool for structure–activity relationship studies was

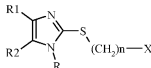
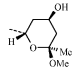
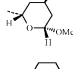
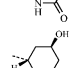
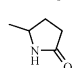
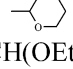
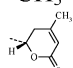
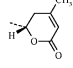
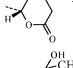
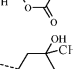
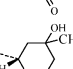
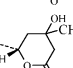
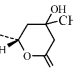
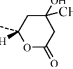
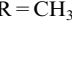

examined for three series of molecules. The first series involves 40 compounds displaying different inhibitory activity (range of 4 pIC_{50} units) for the Acyl-CoA Cholesterol O-Acyl Transferase (ACAT) enzyme (see Tables 1–4) [25–27], which have received considerable attention owing to their cholesterol-lowering and antiatherosclerotic properties [28]. The second set of compounds corresponds to 14 agonists of the 5-hydroxytryptamine 3 receptor (5-HT₃R; see Table 5), a member of a superfamily of ligand-gated ion channel receptors with potential therapeutic properties [29, 30]. Finally, the third series of compounds includes 114 1,2-diarylimidazole compounds [31, 32] acting as inhibitors (covering a range of near 5 pIC_{50} units) of the Cyclooxygenase 2 enzyme (see Tables 6–9), which mediate inflammation processes [33].

Computational details

MST continuum calculations in water and in octanol were performed to obtain the fractional contributions to the octanol/water transfer free energy. Computations were carried out using the semiempirical AM1 [34] version of the MST model [19, 35] implemented in a locally modified version of MOPAC-6 [36]. In all cases the molecular geometry was optimized using the standard geometry optimization procedure implemented in MOPAC-6 before carrying out the MST solvation calculations. Choice of this level of theory was motivated by its low computational cost compared to *ab initio* methods, which enables it to be widely used in the study of large-sized drug-like compounds. For ACAT compounds, the side chain linked to the diphenyl-substituted ring was built up in an extended orientation. For the 5-HT₃R agonists, the molecules in their neutral state were considered, since the ionizable groups are expected to be counterbalanced by suitable interactions with oppositely charged residues in the receptor [37, 38].

Molecular alignment was carried out using our MC-MST program [39]. To this end, molecules were initially fitted by superposing their geometric centers and aligning their hydrophobic dipoles [40]. To refine the relative orientation that maximizes the hydrophobic overlap, 20 different copies of the superposed molecule were generated around the reference molecule by random translational and rotational changes. Then, for each starting

Table 1. Inhibitory activity data (pIC₅₀), calculated octanol/water partition coefficient (log*P*) and global hydrophobic similarity (γ) measured from the fractional contributions to the log*P* for the diphenylimidazole ACAT inhibitors.

Compound ^a	R ₁	R ₂	X	PIC ₅₀ ^b	log <i>P</i> ^c	γ ^d
						
1	C ₆ H ₅	C ₆ H ₅		7.52	0.0	1.00
2	C ₆ H ₅	C ₆ H ₅		7.05	0.3	0.94
3	C ₆ H ₅	C ₆ H ₅		6.21	-1.6	0.61
4	C ₆ H ₅	C ₆ H ₅		6.04	-2.8	0.74
5	C ₆ H ₅	C ₆ H ₅		6.44	-2.3	0.66
6	C ₆ H ₅	C ₆ H ₅		6.68	-0.8	0.93
7	C ₆ H ₅	C ₆ H ₅	CH(OEt) ₂	7.16	-0.1	0.91
8	C ₆ H ₅	C ₆ H ₅	CH ₃	6.14	-1.8	0.93
9	4-F-C ₆ H ₄	4-F-C ₆ H ₄		6.21	-1.2	0.78
10	2-Cl-C ₆ H ₄	2-Cl-C ₆ H ₄		5.77	0.1	0.63
11	4-CH ₃ O-C ₆ H ₄	4-CH ₃ O-C ₆ H ₄		6.38	-2.2	0.80
12	4-CF ₃ -C ₆ H ₄	4-CF ₃ -C ₆ H ₄		6.00	0.8	0.82
13	4-CH ₃ -C ₆ H ₄	4-CH ₃ -C ₆ H ₄		6.77	-1.7	0.78
14	3-Cl-C ₆ H ₄	3-Cl-C ₆ H ₄		6.96	-0.7	0.81
15	3-CH ₃ O-C ₆ H ₄	3-CH ₃ O-C ₆ H ₄		6.24	-1.8	0.79
16	3-CH ₃ -C ₆ H ₄	3-CH ₃ -C ₆ H ₄		7.19	-1.6	0.78
17	C ₆ H ₅	C ₆ H ₄		5.59	-1.7	0.71

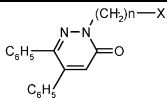
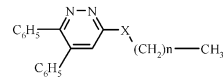
^aR = H and *n* = 1 for all molecules but compounds 17 and 7, which have R = CH₃ and *n* = 2, respectively.

^bData taken from Ref. [25]. IC₅₀ values expressed in M.

^cRelative to compound 1 (log*P* = 7.6).

^dDetermined using compound 1 as reference in the superposition process.

Table 2. Inhibitory activity data (pIC₅₀), calculated octanol/water partition coefficient (log*P*) and hydrophobic similarity (γ) measured from the fractional contributions to the log*P* for the diphenylpyridazine ACAT inhibitors.

Compound	N	X	pIC ₅₀ ^a	log <i>P</i> ^b	γ ^c
					
18	2	CH ₃	3.64	-1.5	0.54
19	3	CH ₃	3.75	-1.0	0.53
20	4	CH ₃	4.18	-0.6	0.53
21	6	CH ₃	4.07	0.5	0.51
22	0	cyclopentyl	3.92	-1.0	0.41
					
23	5	NH	4.62	-0.8	0.49
24	7	NH	4.40	-0.3	0.48
25	8	NH	4.74	0.1	0.47
26	4	O	4.14	-0.6	0.62
27	7	O	3.98	0.9	0.57
28	7	S	3.89	2.0	0.56
29	7	SO	4.04	-3.2	0.27
30	5	SO ₂	4.22	-3.9	0.21
31	6	SO ₂	4.31	-3.5	0.21
32	7	SO ₂	4.44	-3.0	0.20

^aData taken from Refs. [26] and [27]. IC₅₀ values expressed in M.

^bRelative to compound 1 (Table 1).

^cDetermined using compound 1 (Table 1) as reference in the superposition process.

orientation a Metropolis Monte Carlo-based searching algorithm combined with gradient optimization techniques was used to obtain the final alignment. No exploration was made relative internal degrees of freedom, which appears to be a reasonable approximation at least for both 5-HT₃R and COX-2 compounds. The hydrophobic similarity function (Equation 8) was evaluated by using $n=1$ and $\delta=1/2$ (the similarity between molecules was found to be not very sensitive to the values adopted for these parameters, which mainly modulate the convergence process). By using the alignment procedure describe above, which can still be refined in several ways, the limiting step in the evaluation of the MST-based hydrophobic similarity approach presented here lies in the calculation of the atomic contributions to the octanol/water partition coefficient.

Results

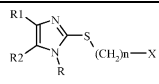
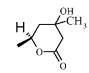
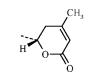
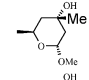
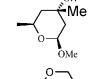
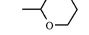
The two first series of compounds (ACAT inhibitors and 5-HT₃R agonists) were used to explore the suitability of the global measure of hydrophobic similarity to align the different compounds and to relate the hydrophobic similarity index with the differences in biological activity. Owing to the presence of well-defined structural moieties in the third series of compounds (COX-2 inhibitors), the structure-activity relationships were examined considering the local measures of hydrophobic similarity.

ACAT inhibitors

These compounds possess an *o*-diphenyl-substituted heteroaromatic (imidazole or pyridazine) ring linked through an alkyl side chain to a variety of capping groups. Within the series of compounds, the linker has different length and in some cases contains functional groups such as >NH, -O-, -S-, >SO or -SO₂-. The capping groups include different chemical entities, such as functionalized lactime or lactame rings, phenyl or methyl, as well as alicyclic compounds. Tables 1 and 2 report the calculated octanol/water partition coefficient, log *P*, and the global hydrophobic similarity index, γ for the series of ACAT inhibitors.

The MST method reproduced the octanol/water partition coefficient with a root-mean square deviation of 0.5 log *P* units for a training set of 75 neutral compounds containing prototypical functional groups [35]. However, the results in Table 1 show some shortcomings of the AM1 method for the accurate prediction of log*P* in certain cases. For instance, replacement of -S- (compound 28) by >SO and -SO₂- makes compounds 29-32 to be too hydrophilic, which can be attributed to the failure of the AM1 method to properly describe the polarity in S=O groups [41]. As a result, the differences in log*P* for those compounds are exaggerated with regard to the values obtained from empirical approaches [42]. Despite the uncertainties in the calculation of the log*P* for compounds with functional groups poorly represented in the AM1 method, the use of fractional contributions to the log*P* should lead to a description of the hydrophobicity less sensitive to those errors and therefore accurate enough to measure the

Table 3. Inhibitory activity data (pIC_{50}), calculated octanol/water partition coefficient ($\log P$) and global hydrophobic similarity (γ) measured from the fractional contributions to the $\log P$ for the diphenylimidazole ACAT inhibitors used in the validation set.

Compound ^a	R ₁	R ₂	X	pIC_{50}^b	$\log P^c$	γ^d
						
33	4-CH ₃ O-C ₆ H ₄	4-CH ₃ O-C ₆ H ₄		6.47	-3.7	0.85
34	3-Cl-C ₆ H ₄	3-Cl-C ₆ H ₄		6.36	-1.1	0.59
35	C ₆ H ₅	C ₆ H ₅		6.55	-0.7	0.92
36	C ₆ H ₅	C ₆ H ₅		7.09	-1.2	0.95
37	C ₆ H ₅	C ₆ H ₅		6.14	-1.0	0.79

^aR = H and $n = 1$ for all molecules but compound 36 which has $n = 2$.

^bData taken from Ref. [25]. IC_{50} values expressed in M.

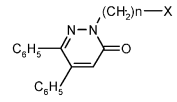
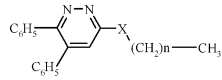
^cRelative to compound 1 (Table 1).

^dDetermined using compound 1 (Table 1) as reference in the superposition process.

similarity between molecules. This is clearly seen in Figure 1, which represents the variation of the biological activity for the ACAT inhibitors in front of the total $\log P$ as well as of the global hydrophobic similarity index (γ). There is no correlation between the $\log P$ values and the inhibitory activity of the ligands (Figure 1; top), even after removal of compounds 29–32, thus

revealing that the biological activity apparently is not related to the total hydrophobicity of the compounds. However, when the molecules are aligned based on their hydrophobic 3D distribution, a reasonable correlation (see Figure 1; bottom) between the inhibitory activity and the hydrophobic similarity index emerges (Equation 13; the correlation coefficient increases up to 0.88

Table 4. Inhibitory activity data (pIC_{50}), calculated octanol/water partition coefficient ($\log P$) and hydrophobic similarity (γ) measured from the fractional contributions to the $\log P$ for the diphenylpyridazine ACAT inhibitors used in the validation set.

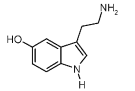
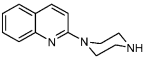
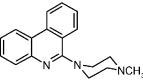
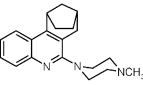
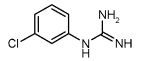
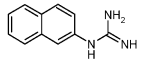
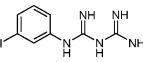
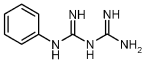
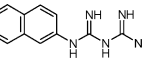
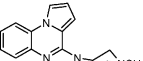
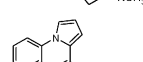
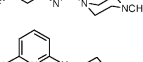
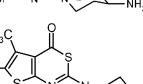
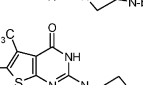
Compound	n	X	pIC_{50}^a	$\log P^b$	γ^c
					
38	5	CH ₃	4.24	0.0	0.23
					
39	8	O	3.74	1.4	0.49
40	8	SO	4.06	-3.1	0.27

^aData taken from Refs. [26] and [27]. IC_{50} values expressed in M.

^bRelative to compound 1 (Table 1).

^cDetermined using compound 1 (Table 1) as reference in the superposition process.

Table 5. Binding activity (pK_i), calculated octanol/water partition coefficient ($\log P$) and hydrophobic similarity (γ) measured from the fractional contributions to the $\log P$ for the 5-HT₃ receptor ligands.

Compound		pK_i^a	$\log P^b$	γ^c
1		6.92	0.0	0.54
2		8.74	1.5	0.87
3		8.72	2.8	0.93
4		9.08	3.3	0.92
5		7.46	1.5	0.70
6		7.60	1.6	0.80
7		7.77	3.5	0.73
8		5.92	3.1	0.70
9		7.92	4.2	0.76
10		9.64	2.1	1.00
11		9.29	3.3	0.97
12		6.99	2.6	0.85
13		6.42	7.4	0.69
14		6.44	5.5	0.68

^aData taken from Ref. [30]. K_i values expressed in M.

^bRelative to compound 1 ($\log P=1.5$).

^cDetermined using compound 1 as reference in the superposition process.

when compounds 29–32 are not included in the regression analysis). Furthermore, consistent predictive results ($r=0.86$) are obtained when Equation 13 is used to validate an external set of eight compounds shown in Tables 3 and 4 (see Figure 1). These findings suggest that, despite the

noise introduced by the uncertainties in the calculated $\log P$, the enrichment in information provided by the use of 3D descriptions of the hydrophobic distribution along the structural skeleton is very important for the prediction of differences in biological activities.

$$pIC_{50} = 4.67\gamma + 2.45 \quad r = 0.84 \quad q^2 = 0.66 \quad (13)$$

The predictive power of the global hydrophobic similarity index is further improved when only the electrostatic fractional contribution to the $\log P$ ($\Delta G_{ele,i}$) is used instead of the total (electrostatic + non-electrostatic) one (ΔG_{w-o}) to calculate the similarity between molecules (Equation. 8), as noted in a Pearson's correlation coefficient of 0.93 (data not shown). The larger discrimination is not unexpected, since the electrostatic component of the transfer free energy is especially sensitive to the chemical differences between compounds. Accordingly, the definition of separate similarity indexes for the electrostatic and non-electrostatic components of the $\log P$ might be valuable to gain insight into the relationship between chemical constituents of compounds and their biological activity.

A graphical inspection of the fractional distributions for selected ACAT inhibitors (see Figure 2) shows that the differences in inhibitory activity can be mainly attributed to (i) an enhancement in the hydrophobicity in the region around the diphenyl-substituted aromatic ring (hydrophobic and hydrophilic regions are shown in blue and red, respectively), which is clearly favored by the presence of the sulfur atom in the side chain attached to the imidazole ring in compound 1, and (ii) the existence of a hydrophilic unit in the capping region of the molecule. The former factor might be related to the binding of the diphenyl-substituted aromatic ring into a highly hydrophobic cavity of the receptor, whereas the latter might be interpreted as the formation of a polar (i.e., hydrogen bond) contacts between the terminal moiety of the compound and specific groups of the receptor. For our purposes here, it is clear that not only compact measures of hydrophobic similarity, but also inspection of the 3D pattern of hydrophobic/hydrophilic contributions can be useful to explore the factors that modulate the binding of a given series of compounds.

Table 6. Inhibitory activity data (pIC_{50}) and local indexes^a of hydrophobic similarity (γ) measured from the fractional contributions to the log P for COX-2 inhibitors used in the training set.

Compound	R1	R2	R3	pIC_{50}^b	γ^A	γ^B	γ^C
----------	----	----	----	---------------------	------------	------------	------------

1	4-SO ₂ Me	4-F	CF ₃	7.00	0.91	0.93	0.68
2	4-SO ₂ Me	H	CF ₃	6.92	0.96	0.90	0.75
3	4-SO ₂ Me	4-Me	CF ₃	6.80	0.95	0.93	0.79
4	4-SO ₂ Me	4-Ome	CF ₃	6.24	0.93	0.87	0.75
5	4-SO ₂ Me	4-NMe ₂	CF ₃	6.15	0.98	0.94	0.76
6	4-SO ₂ Me	4-Sme	CF ₃	6.80	0.85	0.80	0.46
7	4-SO ₂ Me	3-Cl	CF ₃	7.22	0.97	0.91	0.91
8	4-SO ₂ Me	3-F	CF ₃	6.92	0.96	0.93	0.66
9	4-SO ₂ Me	3-Br	CF ₃	7.10	0.97	0.92	0.86
10	4-SO ₂ Me	3-CF ₃	CF ₃	6.68	0.91	0.97	0.85
11	4-SO ₂ Me	3-Sme	CF ₃	6.46	0.94	0.92	0.72
12	4-SO ₂ Me	2-Cl	CF ₃	6.05	0.86	0.90	0.50
13	4-SO ₂ Me	2-F	CF ₃	6.40	0.95	0.92	0.70
14	4-SO ₂ Me	4-Ome-3-F	CF ₃	6.82	0.83	0.91	0.69
15	4-SO ₂ Me	4-Nme ₂ -3-F	CF ₃	6.48	0.96	0.94	0.71
16	4-SO ₂ Me	4-Me-3-Cl	CF ₃	7.52	0.98	0.94	0.93
17	4-SO ₂ Me	4-Me-3-F	CF ₃	6.96	0.91	0.91	0.70
18	4-SO ₂ Me	3-Me-4-F	CF ₃	6.77	0.94	0.93	0.80
19	4-SO ₂ Me	3-Me-4-Cl	CF ₃	7.05	0.95	0.95	0.75
20	4-SO ₂ Me	3-Ome-4-Cl	CF ₃	6.60	0.92	0.86	0.60
21	4-SO ₂ Me	3,4-OCH ₂ O-	CF ₃	6.77	0.95	0.95	0.73
22	4-SO ₂ Me	3,4-diMe	CF ₃	6.48	0.98	0.92	0.83
23	4-SO ₂ Me	3-Ome-5-F	CF ₃	6.02	0.83	0.87	0.78
24	4-SO ₂ Me	3,5-diCl	CF ₃	6.77	0.95	0.92	0.80
25	4-SO ₂ Me	4-Ome-3,5-diF	CF ₃	6.77	0.86	0.86	0.79
26	4-SO ₂ Me	4-Ome-3,5-diCl	CF ₃	6.85	0.94	0.92	0.86
27	4-SO ₂ Me	4-Ome-3,5-diMe	CF ₃	6.14	0.96	0.88	0.78
28	4-SO ₂ Me	4-NMe ₂ -3,5-diCl	CF ₃	6.85	0.94	0.90	0.73
29	4-SO ₂ Me	4-Cl	Me	6.62	0.73	0.89	0.71
30	4-SO ₂ Me	4-Cl	CHF ₂	6.21	0.63	0.92	0.68
31	4-SO ₂ Me	4-Cl	CHO	5.80	0.37	0.93	0.67
32	4-SO ₂ Me	4-Cl	CN	6.64	0.75	0.92	0.67
33	4-SO ₂ Me	4-Cl	Ph	6.62	0.67	0.89	0.71
34	4-SO ₂ Me	4-Cl	CH ₂ OPh(4-Cl)	7.52	0.70	0.88	0.49
35	4-SO ₂ Me	4-SMe,3-Cl	CF ₃	7.40	0.85	0.92	0.77
36	4-SO ₂ Me	4-Cl	CH ₂ SPh(4-Cl)	7.30	0.61	0.85	0.41
37	4-SO ₂ Me	4-Cl	CH ₂ OH	5.08	0.18	0.92	0.69
38	4-SO ₂ Me	CH ₂ Ome	CF ₃	4.17	0.88	0.93	0.81
39	4-SO ₂ Me	4-Cl	CH ₂ SO ₂ Me	4.00	0.22	0.88	0.38
40	4-SO ₂ Me	4-Cl	CO ₂ NEt ₂	4.00	0.43	0.87	0.31
41	4-SO ₂ Me	4-F	CH ₃	4.00	0.51	0.86	0.31
42	4-SO ₂ Me	4-Cl	CH ₂ SMe	6.49	0.65	0.90	0.70

Table 6. Continued

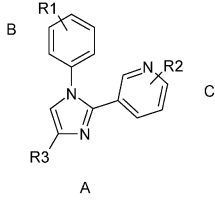
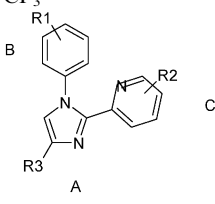
Compound	R1	R2	R3	pIC ₅₀ ^b	γ ^A	γ ^B	γ ^C
43	4-SO ₂ NH ₂	4-Cl	CF ₃	8.00	0.92	0.66	0.65
44	4-SO ₂ NH ₂	H	CF ₃	7.40	0.91	0.65	0.74
45	4-SO ₂ NH ₂	4-Me	CF ₃	7.40	0.91	0.65	0.77
46	4-SO ₂ NH ₂	3-Cl	CF ₃	8.10	0.98	0.95	0.92
47	4-SO ₂ NH ₂	3-F	CF ₃	7.52	0.45	0.50	0.87
48	4-SO ₂ NH ₂	3-Br	CF ₃	8.15	0.99	0.97	0.85
49	4-SO ₂ NH ₂	3-Me	CF ₃	7.52	0.90	0.58	0.82
50	4-SO ₂ NH ₂	2-F	CF ₃	7.00	0.85	0.69	0.67
51	4-SO ₂ NH ₂	2-Me	CF ₃	6.70	0.83	0.70	0.66
52	4-SO ₂ NH ₂	4-OMe-3-Cl	CF ₃	7.70	0.95	0.99	0.82
53	4-SO ₂ NH ₂	4-OMe-3-Br	CF ₃	7.52	0.90	0.98	0.66
54	4-SO ₂ NH ₂	4-SMe-3-Cl	CF ₃	8.00	0.92	0.98	0.73
55	4-SO ₂ NH ₂	4-Me-3-Cl	CF ₃	8.52	1.00	1.00	1.00
56	4-SO ₂ NH ₂	3,4-diF	CF ₃	7.52	0.91	0.97	0.85
57	4-SO ₂ NH ₂	3-Me-5-Cl	CF ₃	7.40	0.95	0.95	0.67
58	4-SO ₂ NH ₂	3-Me-5-F	CF ₃	7.52	0.93	0.94	0.80
59	4-SO ₂ NH ₂	4-OMe-3,5-diF	CF ₃	7.52	0.89	0.94	0.78
60	4-SO ₂ NH ₂	3-OMe-5-F	CF ₃	6.34	0.99	0.99	0.88
							
61	4-SO ₂ Me	H	CF ₃	5.77	0.93	0.95	0.55
62	4-SO ₂ Me	2-Me	CF ₃	5.02	0.90	0.90	0.52
63	4-SO ₂ Me	6-OMe	CF ₃	5.92	0.87	0.81	0.46
64	4-SO ₂ Me	5-Br	CF ₃	6.02	0.91	0.93	0.32
65	4-SO ₂ Me	4-Me	CF ₃	4.27	0.71	0.84	0.46
66	4-SO ₂ Me	H	Me	4.10	0.62	0.87	0.35
67	4-SO ₂ Me	H	CH ₂ OH	3.07	0.47	0.85	0.28
68	4-SO ₂ NH ₂	H	CF ₃	6.36	0.98	0.96	0.68
69	4-SO ₂ NH ₂	2-Me	CF ₃	5.55	0.89	0.94	0.50
70	4-SO ₂ NH ₂	6-Me	CF ₃	6.54	0.78	0.96	0.58
71	4-SO ₂ NH ₂	4-Me	CF ₃	4.29	0.89	0.95	0.43
72	4-SO ₂ NH ₂	5-Br	CF ₃	6.47	0.93	0.96	0.80
							
73	4-SO ₂ Me	H	CF ₃	5.82	0.88	0.81	0.58
74	4-SO ₂ Me	6-Me	CF ₃	5.54	0.83	0.83	0.50
75	4-SO ₂ Me	5-Me	CF ₃	5.89	0.89	0.93	0.51
76	4-SO ₂ Me	3-Me	CF ₃	5.24	0.80	0.72	0.59

Table 6. Continued

77	4-SO ₂ NH ₂	6-Me	CF ₃	6.38	0.81	0.95	0.49
78	4-SO ₂ NH ₂	5-Me	CF ₃	6.14	0.82	0.72	0.45
79	4-SO ₂ NH ₂	4-Me	CF ₃	6.36	0.84	0.60	0.51
80	4-SO ₂ NH ₂	3-Me	CF ₃	5.80	0.78	0.73	0.59

Labeling of the three ring units (A–C) mentioned in the text is shown.

^aDetermined using compound 55 as reference.

^bIC₅₀ values expressed in M.

Table 7. Inhibitory activity data (pIC₅₀) and local indexes^a of hydrophobic similarity (γ) measured from the fractional contributions to the log*P* for COX-2 inhibitors used in the training set. Labeling of the three ring units (A–C) mentioned in the text is shown.

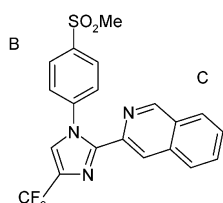
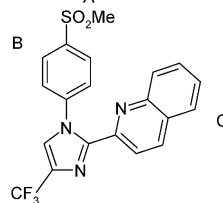
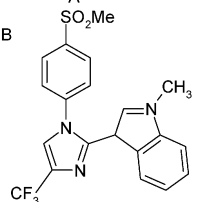
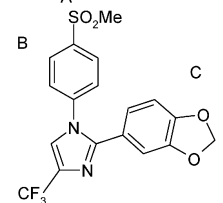
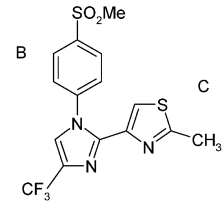
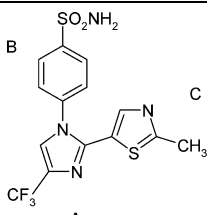
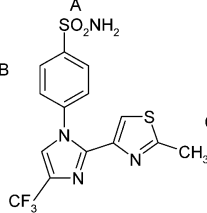
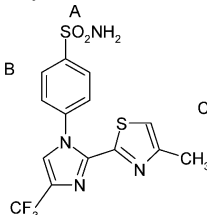
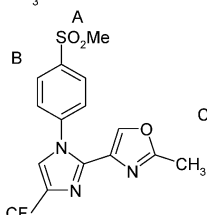
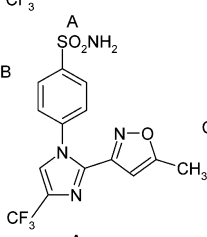
Compound		pIC ₅₀ ^b	γ^A	γ^B	γ^C
81		5.92	0.91	0.80	0.55
82		6.20	0.90	0.92	0.53
83		5.96	0.95	0.90	0.59
84		6.55	0.95	0.95	0.73
85		6.03	0.91	0.87	0.49

Table 7. Continued.

Compound		pIC ₅₀ ^b	γ ^A	γ ^B	γ ^C
86		6.28	0.85	0.70	0.52
87		6.37	0.82	0.82	0.29
88		6.96	0.80	0.86	0.33
89		5.38	0.92	0.86	0.46
90		6.39	0.41	0.90	0.17

^aDetermined using compound 55 as reference.^bIC₅₀ values expressed in M.

5-HT₃ receptor agonists

Compared to the preceding series of compounds, the structure of 5-HT₃R agonists is chemically more diverse, including a variety of functionalized (hetero)aromatic rings linked to different polar moieties. Thus, these compounds represent a suitable test, complementary to the analysis of

ACAT inhibitors, to evaluate the applicability of the global hydrophobic similarity index.

Table 5 shows the corresponding chemical structures of the compounds in the series of 5-HT₃R agonists, as well as their calculated octanol/water partition coefficient, log *P*, and global hydrophobic similarity index, γ. Again, the log *P* is not able to explain the differences in binding affinity for

Table 8. Inhibitory activity data (pIC_{50}) and local indexes^a of hydrophobic similarity (γ) measured from the fractional contributions to the $\log P$ for COX-2 inhibitors used in the validation set.

Compound	R ₁	R ₂	R ₃	pIC_{50}^b	γ^A	γ^B	γ^C
----------	----------------	----------------	----------------	---------------------	------------	------------	------------

91	4-SO ₂ Me	4-Cl	CF ₃	6.96	0.97	0.93	0.66
92	4-SO ₂ Me	2-Me	CF ₃	6.10	0.81	0.93	0.72
93	4-SO ₂ Me	4-F	CF ₃	5.23	0.91	0.93	0.71
94	4-SO ₂ Me	3-Nme ₂	CF ₃	5.49	0.93	0.91	0.79
95	4-SO ₂ Me	3-NHMe	CF ₃	6.04	0.89	0.95	0.44
96	4-SO ₂ Me	4-OMe-3-Cl	CF ₃	6.89	0.95	0.92	0.60
97	4-SO ₂ Me	4-NMe ₂ -3-Cl	CF ₃	6.49	0.94	0.93	0.62
98	4-SO ₂ Me	3-NMe ₂ -4-Cl	CF ₃	5.98	0.98	0.93	0.61
99	4-SO ₂ Me	3,4-diF	CF ₃	6.92	0.87	0.91	0.61
100	4-SO ₂ Me	3-Me-5-F	CF ₃	6.96	0.96	0.94	0.79
101	4-SO ₂ Me	4-OMe-3,5-diBr	CF ₃	7.05	0.94	0.92	0.72
102	4-SO ₂ Me	4-Cl	CH ₂ F	6.39	0.68	0.91	0.69
103	4-SO ₂ Me	4-Cl	CO ₂ Et	5.24	0.28	0.93	0.68
104	4-SO ₂ Me	4-Cl	CH ₂ OMe	5.43	0.41	0.89	0.71
105	4-SO ₂ Me	4-Cl	CH ₂ CN	5.81	0.85	0.91	0.68
106	4-SO ₂ NH ₂	4-F	CF ₃	8.00	0.91	0.65	0.71
107	4-SO ₂ NH ₂	4-Ome-3-F	CF ₃	7.52	0.94	0.96	0.90

108	4-SO ₂ Me	5-OMe	CF ₃	4.43	0.64	0.90	0.48
109	4-SO ₂ Me	6-Me	CF ₃	5.74	0.87	0.88	0.51

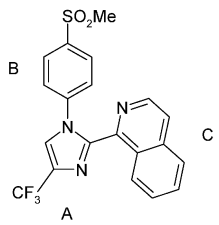
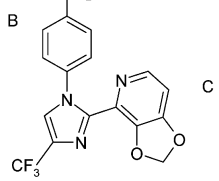
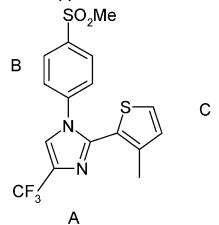
110	4-SO ₂ Me	4-Me	CF ₃	6.28	0.91	0.86	0.65
111	4-SO ₂ Me	H	CN	4.61	0.87	0.90	0.62

Labeling of the three ring units (A–C) mentioned in the text is shown.

^aDetermined using compound 55 as reference.

^b IC_{50} values expressed in M.

Table 9. Inhibitory activity data (pIC₅₀) and local indexes^a of hydrophobic similarity (γ) measured from the fractional contributions to the log *P* for COX-2 inhibitors used in the validation set.

Compound	pIC ₅₀ ^b	γ ^A	γ ^B	γ ^C
112	5.77	0.88	0.95	0.50
				
113	6.33	0.89	0.87	0.70
				
114	5.96	0.89	0.90	0.35
				

Labeling of the three ring units (A-C) mentioned in the text is shown.

^aDetermined using compound 55 as reference.

^bIC₅₀ values expressed in M.

the 5-HT₃R compounds (see Figure 3). However, a reasonably good correlation is found between the binding affinity and the global hydrophobic similarity index (Equation 14; see Figure 3). The existence of such a correlation is remarkable keeping in mind that previous studies have related the activity of these compounds with the electrostatic potential distribution [37, 38], showing that the fractional contributions implicitly incorporates information on the electrostatic potential of the molecules.

$$\text{pK}_i = 7.82\gamma + 1.63 \quad r = 0.83 \quad q^2 = 0.63 \quad (14)$$

Inspection of the atomic contributions to the log *P* (Figure 4) reflects a series of key structural features for the 5-HT₃R agonists. First, the presence of a hydrophilic region due to the ionizable group, which would contact a negatively charged group in the receptor. Second, the occurrence of a

hydrophilic region in the aryl ring that is directly attached to the piperidine or guanide unit, which has been hypothesized to mediate binding through the formation of a hydrogen-bond interaction [30]. Finally, a hydrophobic region extending beyond the aryl ring bonded to the ionizable unit, as found in those compounds with a quinoline unit. These features reflect the basic trends of the pharmacophore model proposed from previous structure–activity relationship studies [37], and support the hypothesis that two distinct ‘aryl’ interactions are crucial for the agonist activity of this family of compounds [30]. Thus, the large difference in binding affinity of biguanide compounds 7 and 8 (*K*_i’s of 17 and 1200 nM, respectively), which merely differs by the presence of a chlorine atom, can be related to the extension of the hydrophobicity around the aryl region and to the larger negative electrostatic surface found in the former compound (Table 5 and Figure 4), which reflects

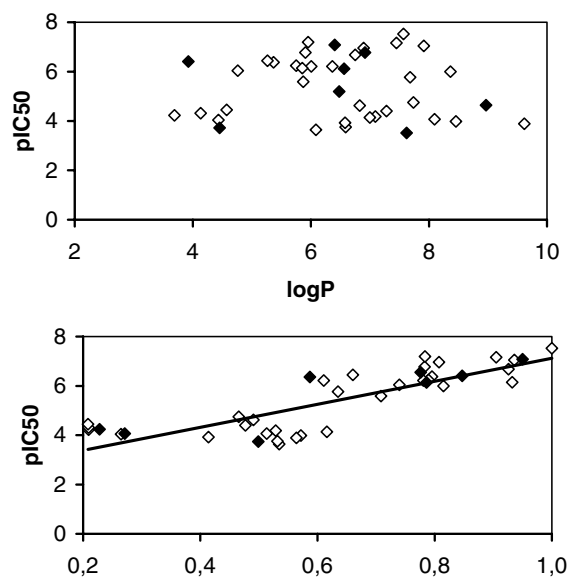


Figure 1. Representation of the inhibitory activity (expressed as pIC_{50} data) in front of the calculated octanol/water partition coefficient ($\log P$; top) and the hydrophobic similarity index (γ ; bottom) for the series of ACAT inhibitors used in the training (white) and validation (black) subsets.

the trends (hydrophobicity of the quinoline ring and negative electrostatic isocontour) found in compound 10 (i.e., the most active molecule). Therefore, the chlorine atom mimics the benzene ring, thus explaining the similar binding exhibited by compounds 5 ($K_i = 35$ nM) and 6 ($K_i = 25$ nM), as well as by compounds 7 ($K_i = 17$ nM) and 9 ($K_i = 12$ nM).

COX-2 inhibitors

The suitability of the local hydrophobic similarity index (see Equations 10–12) to explore structure–activity relationships is examined for a series of 114 COX-2 inhibitors, whose structure can be partitioned in three units: (i) the central imidazole ring, which bears different substituents at position 4 (ring A), (ii) the sulfone/sulfonamide substituted benzene attached to the imidazole nitrogen (ring B), and (iii) the other substituted or unsubstituted benzene ring (ring C). Despite the high structural similarity between compounds, it is worth noting that subtle rearrangements in the COX-2 binding site can occur depending on the chemical features of the inhibitor [43], thus

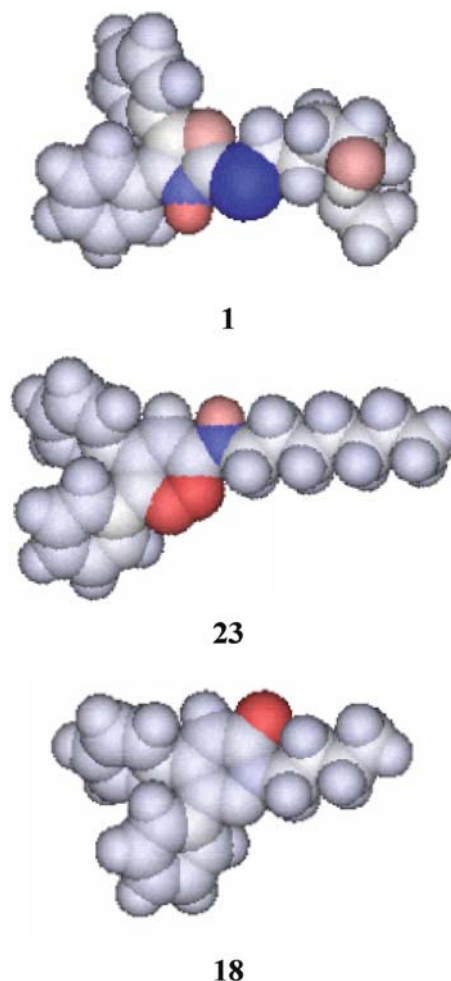


Figure 2. Representation of the atomic contributions to the octanol/water transfer free energy for ACAT inhibitors (from top to bottom) 1 ($pIC_{50} = 7.52$), 23 ($pIC_{50} = 4.62$) and 18 ($pIC_{50} = 3.75$). Hydrophobic/hydrophilic regions are shown in blue/red.

making this series of compounds to be a challenging test.

Tables 6 and 7 report the local hydrophobic similarity index, γ^k ($k = A, B$, and C) for a subset of 90 COX-2 inhibitors (taken from [44]) used as training data to derive the parameters α_k , which were determined by fitting to the biological data (Equation 12). The predictive ability of the fitted equation was then checked for a subset of 24 compounds (Tables 8 and 9; [44]). The indexes γ_k were determined by using the structural alignment reported previously in the literature [45] without further refinement, since test calculations revealed

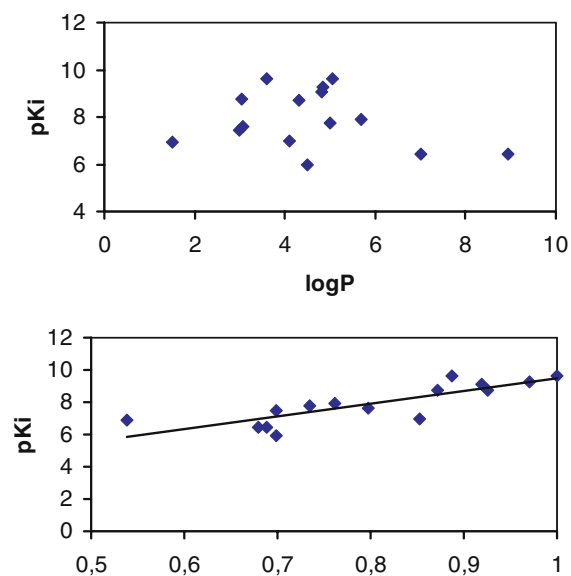


Figure 3. Representation of the binding affinities (pK_i) in front of the calculated octanol/water partition coefficient ($\log P$; top) and the hydrophobic similarity index (γ ; bottom) for the series of 5-HT₃R agonists.

negligible changes in the relative orientation of the molecules when they were allowed to move in order to maximize the hydrophobic similarity.

Comparison of the differences in inhibitory activity with the indexes γ_k ($k = A, B$, and C) yields to Equation 15. The coefficients α_k for rings A and C and the independent term were determined with statistical significance ($p < 0.003$). However, this was not true for ring B. In fact, the predictive ability of the regression equation is little affected upon exclusion of the index γ_B (see Equations. 15 and 16). This finding reflects the dominant role played by the interaction between the sulfone/sulfonamide oxygen atoms and the guanidinium moiety of Arg513 [43], which masks the differential binding effects due to replacement of the methyl group by an amino unit. Moreover, Equation 16 predicts with a similar degree of confidence ($r = 0.64$) the biological activity for the subset of compounds included in the validation test (see Figure 5).

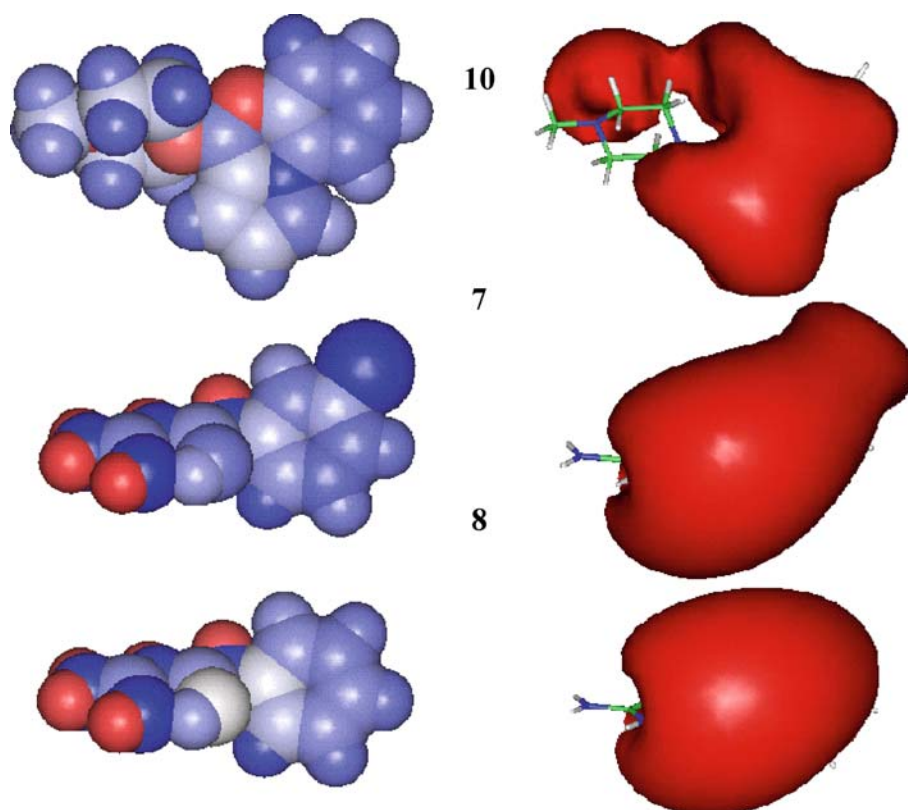


Figure 4. Representation (left) of the atomic contributions to the octanol/water transfer free energy for 5-HT₃R agonists (from top to bottom) 10 ($pK_i = 9.64$), 7 ($pK_i = 7.77$) and 8 ($pK_i = 5.92$). Hydrophobic/hydrophilic regions are shown in blue/red. Isocontour plots (right) of the negative electrostatic potential for molecules 10, 7 and 8.

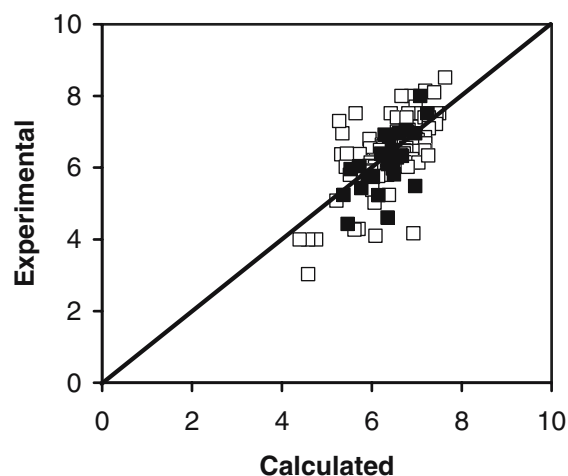


Figure 5. Representation of the experimental versus calculated inhibitory activities (pIC_{50}) for the compounds used in the training (white) and validation (black) subsets.

$$pIC_{50} = 1.66(\pm 0.54)\gamma^A - 1.09(\pm 0.84)\gamma^B + 3.23(\pm 0.51)\gamma^C + 3.93(\pm 0.78) \\ n = 90 \quad r = 0.71 \quad q^2 = 0.44 \quad (15)$$

$$pIC_{50} = 1.57(\pm 0.54)\gamma^A + 3.18(\pm 0.52)\gamma^C + 3.09(\pm 0.44) \quad n = 90 \quad r = 0.70 \\ q^2 = 0.43 \quad (16)$$

The preceding results exhibit only moderate predictive ability for the set of 114 COX-2 inhibitors. However, this is achieved considering only the hydrophobic properties of the compounds, which reveals the relevant role played by hydrophobic forces in the binding to COX-2. This finding agrees with the results found in COMSIA studies, which points out a substantial increase of predictive ability (enlargement of the cross-validated correlation coefficient from 0.49 to 0.75) upon addition of the hydrophobic field to the steric + electrostatic ones [44].

The role played by hydrophobicity in modulating the activity of these compounds (Equation 16) can be examined from the crystal structure of murine COX-2 complexed to celecoxib (PDB entry 1cx2 [46]). Equation 16 shows that the inhibitory potency increases as the local similarity for rings A

and C relative to the most active compound (55; see Table 8) becomes larger. In the reference compound the imidazole ring (A) bears a CF_3 group at position 4, which has a fractional $\log P$ contribution of 1.14. In the crystal structure ring A fits a hydrophobic pocket formed by Val116, Val349, Tyr355, Leu 359 and Leu531, where only Arg120 introduces a strong electrostatic field. The presence of the CF_3 substituent, therefore, permits to maintain the interaction with the guanidium group of Arg120, but to satisfy the van der Waals contacts with the hydrophobic residues in the binding pocket, as recently confirmed by free energy calculations [43]. Thus, the introduction of polar groups, such as CHO (31), CH_2OH (37,67), CH_2SO_2Me (39) and CO_2NEt_2 (40), decreases the hydrophobic similarity index γ_A , which justifies the reduced activity of these compounds.

As expected from the large chemical diversity found in ring C for the series of compounds, the main contribution to the inhibitory activity (Equation 16) comes from the local hydrophobic similarity index γ_C . Ring C also fits a hydrophobic pocket mainly composed of residues Leu 384, Tyr385, Trp387 and Phe518, which agrees with the lipophilic nature of the 3-chloro,4-methylbenzene unit (fractional $\log P$ contribution of 3.1) in the reference compound. Replacement by more polar rings, such as pyridine derivatives (61–80) or other heteroaromatic rings (81–90), reduce the hydrophobic similarity, thus lowering the inhibitory potency. These findings also agree with previous COMFA results, which identified regions with favorable lipophilic influence near the substituent at position 4 of the benzene ring [45].

Final remarks

Drug-receptor interactions involve fundamentally the same intermolecular forces that modulate partitioning of a solute between water and an immiscible organic phase. Accordingly, the development of methods that provide an accurate representation of the 3D pattern of hydrophobic/hydrophilic regions can be valuable in drug design studies. The preceding results suggest that measures of hydrophobic similarity can be a useful tool to complement molecular similarity studies performed on the basis of electrostatic and steric descriptors. In particular, graphical display of the

fractional hydrophobic contributions can be used to identify pharmacophore patterns and to reveal regions in the molecular skeleton with a large hydrophobic dissimilarity. Moreover, the degree of similarity can be quantified by means of the global hydrophobic similarity index, which can be useful to align molecules and to explore structure–activity relationships. Finally, for structurally related molecules, where different constituent units can be identified, measures of the local hydrophobic similarity can be valuable to gain deeper insight into the hydrophobic complementarity expected for the binding of ligands to a common receptor. This information, in turn, might be valuable to refine scoring functions in docking studies.

Compared to methods based on empirical fragment contributions, the MST method provides fractional contributions to the lipophilicity that incorporate the influence of the whole molecule in the contribution of a given atom with only a small computational effort. Moreover, they do not depend on the existence of suitable parameters for new chemical groups, which might not be present in the empirical databases. Taken together, present results suggest that the MST-based fractional analysis, in conjunction with measures of hydrophobic similarity, can be a valuable tool in drug design studies.

Acknowledgments

Prof. P. Chavatte is kindly acknowledged for providing the geometries of the COX-2 inhibitors. We are also indebted to Dr. C. Curutchet for technical assistance. We thank the Ministerio de Ciencia y Tecnología for financial support (Grant Nos. SAF2002–04282, BIO2003–06848 and GEN2001–4758) and the Centre de Supercomputació de Catalunya for computational facilities. J.M.M. thanks a fellowship from the Departament d'Universitat, Recerca i Societat de la Informació, and S.P. thanks the CEPBA for financial support.

References

- Lengauler, T. and Rarey, M., *Curr. Opt. Struct. Biol.*, 6 (1996) 402.
- Johnson, M.A. and Maggiora, G.M. (Eds.) *Concepts and Applications of Molecular Similarity*. Wiley, New York, 1990.
- Hagadone, T.R., *J. Chem. Inf. Comput. Sci.*, 32 (1992) 515.
- Jakes, S.E. and Willett, P., *J. Mol. Graphics*, 4 (1986) 12.
- VanDrie, J.H., Weininger, D. and Martin, Y.C., *J. Comput.-Aided Mol. Design*, 3 (1989) 225.
- Carbó-Dorca, R., Robert, D., Amat, L., Gironés, X. and Besalú, E. *Lecture Notes in Chemistry Vol 7*. Springer, Berlin, 2000.
- Hodgkin, E.E. and Richards W.G., *Int J. Quantum Chem., Quantum Biol. Symp.*, 14 (1987) 105.
- Klebe, G., Mietzner, T. and Weber, F., *J. Comput.-Aided Mol. Design*, 8 (1994) 751.
- Mestres, J., Rohrer, D.C. and Maggiora, G.M., *J. Comput. Chem.*, 18 (1997) 934.
- Cramer, R.D., III, Patterson, D.E. and Bunce, J.D., *J. Am. Chem. Soc.*, 110 (1988) 5959.
- Palm, K., Luthman, K., Ungell, A.L., Strandlund, G., Begi, F., Lundahl, P. and Artursson, P., *J. Med. Chem.*, 41 (1998) 5–382.
- Kantola, A., Villar, H.O. and Loew, G.H., *J. Comput. Chem.*, 12 (1991) 681.
- Wade, R.C., Clark, K.J. and Goodford, P.J., *J. Med. Chem.*, 36 (1993) 140.
- Jäger, R., Kast, S.M. and Brickmann, J., *J. Chem. Inf. Comput. Sci.*, 43 (2003) 237.
- Heiden, F.W., Moeckel, G. and Brickmann, J., *J. Comput.-Aided Mol. Design*, 7 (1993) 503.
- Carrupt, P., Testa, B. and Gaillard, P., 1997 In Lipkowitz, K.B. and Boyd, D.B., (Eds.), *Reviews in Computational Chemistry*, Vol. 11. Wiley-VCH, New York, 1997, pp. 241–315.
- Croizet, F., Langlois, M.H., Dubost, J.P., Braquet, P., Audry, E., Dallet, P. and Colleter, J.C., *J. Mol. Graphics*, 8 (1990) 153.
- Muñoz, J., Barril, X., Hernández, B., Orozco, M. and Luque, F.J., *J. Comput. Chem.*, 23 (2002) 554.
- Curutchet, C., Orozco, M. and Luque, F.J., *J. Comput. Chem.*, 22 (2001) 1180.
- Miertus, S., Scrocco, E. and Tomasi, J., *Chem. Phys.*, 55 (1981) 117.
- Luque, F.J., Bofill, J.M. and Orozco, M., *J. Chem. Phys.*, 103 (1995) 10183.
- Luque, F.J., Barril, X. and Orozco, M., *J. Comput.-Aided Mol. Des.*, 13 (1999) 139.
- Muñoz, J., Barril, X., Luque, F.J., Gelpí, J.L. and Orozco, M., In Carbó-Dorca, R., Gironés, G. and Mezey, P.G. (Eds.), *Fundamentals of Molecular Similarity*, Vol. 4 Kluwer, New York, 2001, pp. 143–168.
- Carbó, R., Leyda, A. and Arnau, M., *Int. J. Quantum Chem.*, 17 (1980) 1185.
- Harris, N.V., Smith, C., Ashton, M.J., Bridge, A.W., Bush, R.C., Coffee, E.C.J., Dron, D.I., Harper, M.F., Lythgoe, D.J., Newton, C.G. and Riddell, D., *J. Med. Chem.*, 35 (1992) 4384.
- Giovanconi, M.P., Dal Piaz, V., Kwon, B.-M., Kim, M.-K., Kim, Y.-K., Toma, L., Barlocco, D., Bernini, F. and Canavesi, M., *J. Med. Chem.*, 44 (2001) 4292.
- Toma, L., Giovanconi, M.P., Dal Piaz, V., Kwon, B.-M., Kim, Y.-K., Gelain, A. and Barlocco, D., *Heterocycles*, 57 (2001) 39–46.
- Roth, B.D., *Drug Disc. Today*, 3 (1998) 19.
- Morreale, A., Iriepa, I. and Gálvez, E., *Curr. Med. Chem.*, 9 (2002) 99.

30. Parihar, H.S. and Kirschbaum, K.S., *Bioorg. Med. Chem. Lett.*, 12 (2002) 2743.
31. Khana, I.K., Weier, R.M., Yu, Y., Xu, X.D., Koszyk, F.J., Collins, P.W., Koboldt, C.M., Veenhuizen, A.W., Perkins, W.E., Casler, J.J., Masferrer, J.L. and Zhang, Y.Y., *J. Med. Chem.*, 40 (1997) 1634.
32. Khana, I.K., Yu, Y., Huff, R.M., Weier, R.M., Xu, X., Koszyk, F.J., Collins, P.W., Cogburn, J.N., Isakson, P.C., Koboldt, C.M., Masferrer, J.L., Perkins, W.E., Seibert, K., Veenhuizen, A.W., Yuan, J., Yang, D.C. and Zhang, Y.Y., *J. Med. Chem.*, 43 (2000) 3168.
33. Mantri, P. and Witiak, D., *Curr. Med. Chem.*, 1 (1994) 328.
34. Dewar, M.J.S., Zebisch, E.G., Healy, E.F. and Stewart, J.J.P., *J. Am. Chem. Soc.*, 107 (1995) 3902.
35. Curutchet, C., Salichs, A., Barril, X., Orozco, M. and Luque, F.J., *J. Comput. Chem.*, 24 (2003) 32.
36. MOPAC6.0. Version locally modified by Luque, F.J. and Orozco, M. (Univ. Barcelona).
37. Capelli, A., Anzini, M., Vomero, S., Canullo, L., Mennuni, L., Makovec, F., Doucet, E., Hamon, M., Menzini, M.C., De Benedetti, P.G., Bruni, G., Romero, G. and Donati, A., *J. Med. Chem.*, 42 (1999) 1556.
38. Modica, M., Santagati, M., Guccione, S., Santagati, A., Russo, F., Cagnotto, A., Goegan, M. and Mennini, T., *Eur. J. Med. Chem.*, 36 (2001) 287.
39. Colominas, C., Luque, F.J. and Orozco, M., *J. Comput. Chem.*, 7 (1999) 665.
40. Barril, X., Muñoz, J., Luque, F.J. and Orozco, M., *Phys. Chem. Chem. Phys.*, 2 (2000) 4897.
41. Stewart, J.J.P., *J. Comput. Chem.*, 10 (1989) 221.
42. Wang, R., Fu, Y. and Lai, L., *J. Chem. Inf. Comput. Sci.*, 37 (1997) 615.
43. Soliva, R., Almansa, C., Kalko, S.G., Luque, F.J. and Orozco, M., *J. Med. Chem.*, 46 (2003) 1372.
44. Desiraju, G.R., Gopalakrishnan, B., Jetti, R.K.R., Nagaraju, A., Raveendra, D., Sarma, J.A.R.P., Sobhia, M.E. and Thilagavathi, R., *J. Med. Chem.*, 45 (2002) 4847.
45. Chavatte, P., Yous, S., Marot, C., Baurin, N. and Lesieur, D., *J. Med. Chem.*, 44 (2001) 3223.
46. Kurumbail, R.G., Stevens, A.M., Gierse, J.K., McDonald, J.J., Stegeman, R.A., Pak, J.Y., Didelhaus, D., Miyashiro, J.M., Penning, T.D., Seibert, K., Isakson, P.C. and Stallings, W.C., *Nature*, 384 (1996) 644.